Functional Consequences of Differences in Canopy Phenology for the Carbon Budgets of Two Cool-Temperate Forest Types: Simulations Using the NCAR/LSM Model and Validation Using Tower Flux and Biometric Data

SAITOH Taku M.[1]*, NAGAI Shin[2], YOSHINO Jun[3], MURAOKA Hiroyuki[1], SAIGUSA Nobuko[4] and TAMAGAWA Ichiro[1]

[1] River Basin Research Center, Gifu University, 1-1 Yanagido, Gifu 501-1193, Japan
[2] Research Institute for Global Change, Japan Agency for Marine-Earth Science and Technology, 3173-25 Showa-machi Kanazawa-Ku, Yokohama 236-0001, Japan
[3] Graduate School of Engineering, Gifu University, 1-1 Yanagido, Gifu 501-1193, Japan
[4] Center for Environmental Biology and Ecosystem Studies, National Institute for Environmental Studies, 16-2 Onogawa, Tsukuba 305-8506, Japan

Abstract

We quantified the sensitivity of estimated carbon budgets in Japanese evergreen coniferous and deciduous broad-leaved forests using NCAR/LSM simulations under two climatic conditions: the relatively warm end of the cool-temperate zone (i.e., 800 m a.s.l., annual average temperature of 9.4°C, annual average precipitation of 1700 mm), and the relatively cold end of this zone (i.e., 1420 m a.s.l., 7.2°C, and 2400 mm). To improve the model's performance for both forests, we modified parameters such as biomass and plant area index (PAI) based on measured values and calibrated the model using field-measured tower flux and biometric data at two AsiaFlux sites near Takayama City, Japan. The seasonal patterns and annual cumulative values of gross primary production (GPP), ecosystem respiration (RE), and net ecosystem production (NEP) predicted by the model agreed well with field measurements at the two sites. Our sensitivity analysis of the impact of growing period length on the carbon budget in the deciduous broad-leaved forest showed that GPP and NEP increased by 12.7% and 48.0%, respectively, when we considered the temperature dependency of the growing period length. In simulations under both climatic conditions, NEP peaked between April and June in the evergreen coniferous forest, and between July and September in the deciduous broad-leaved forest. The different seasonal patterns of NEP between the two forest types were determined primarily by differences in GPP that resulted from differences in PAI from April to June. The annual values of GPP, RE, and light-use efficiency were clearly greater in the evergreen coniferous forest than in the deciduous broad-leaved forest. Our simulation results suggest that the evergreen coniferous forest has higher metabolic activity than the deciduous broad-leaved forest in this region due to its larger biomass.

Key words: carbon budget, deciduous broad-leaved forest; evergreen coniferous forest; modeling

Introduction

Quantification of carbon budgets and their responses to environmental changes in several forest types will be crucial for predicting future carbon cycling under changing climate (e.g., Bonan 2008). The evergreen coniferous and deciduous broad-leaved forests are dominant forest types in Far East Asia (Ito 2008). Because these forests are expected to experience broad environmental fluctuations over seasons and years under a range of geographical and climatic conditions, analyses of the functional consequences of their different canopy characteristics for ecosystem carbon gain would provide deeper insights into the possible influence of climate change. The carbon budget of a forest ecosystem consists mainly of photosynthetic CO_2 uptake and respiratory CO_2 release, and ecophysiological regulation of the CO_2 cycle is largely responsible for the environmental responses of ecosystem-scale carbon budgets (e.g., Muraoka and Koizumi 2009; Muraoka *et al.* 2010). Quantification of the carbon budget of forest ecosystems has been attempted using eddy-covariance measurements of the CO_2 flux around a forest tower (e.g., Saigusa *et al.* 2005) and biometric analysis of vegetation, which provided a more detailed understanding of carbon cycling in the associated ecosystems (Ohtsuka *et al.* 2007).

Flux data measured from towers provide components of the carbon budget such as gross primary production (GPP), ecosystem respiration (RE), and net ecosystem exchange (NEE = –NEP, where NEP is net ecosystem production) (Baldocchi 2008). Biometric data provide components of the carbon budget such as NEP, net primary production (NPP), soil respiration (R_{soil}), heterotrophic respiration (R_h), and root respiration (R_{root}) (Litton *et al.* 2007). In addition to these *in situ* measurments, modeling analysis is useful for examining the ecophysiological and micrometeorological processes that occur in ecosystems and the integrated effects of these phenomena on

(Received; Sep. 21, 2011: Accepted; Jan. 5, 2012) ∗ Corresponding author: taku@green.gifu-u.ac.jp

carbon budgets. These kinds of analyses can deepen our understanding of carbon dynamics from both mechanistic (process-based simulations) and empirical (plant- or stand-scale observations) perspectives, especially in terms of the responses of carbon budgets to changes in climatic variables (e.g., Ito *et al.* 2005; Sitch *et al.* 2008).

The monsoon climate that characterizes Far East Asia differs from the dominant climates of Europe, North America, and South America (Kim *et al.* 2006; Yu *et al.* 2006; Saigusa *et al.* 2008). To monitor ecosystem carbon budgets in widely areas, Asian researchers require validated model simulations based on a combination of tower flux and biometric data at a range of forest sites. Some previous studies conducted these validations at individual sites in Far East Asia (e.g., Ito *et al.* 2007; Toda *et al.* 2011; Xue *et al.* 2011). However, to clarify and understand the differences in carbon budgets between evergreen coniferous and deciduous broad-leaved forests and the major causes of these differences, it will be necessary to compare two or more ecosystems. Previous studies have described the differences in carbon budgets among several terrestrial ecosystems using model simulations that were calibrated using either tower flux data or biometric measurement data (Ito 2008; Ichii *et al.* 2010; Ueyama *et al.* 2010; Sasai *et al.* 2011). However, we found no examples of comparisons of carbon budgets between two forest types using a model calibrated using both data types.

To provide such a comparison, we performed a long-term, continuous field study using both tower flux and biometric measurements in an evergreen coniferous forest at the AsiaFlux TKC site (Lee *et al.* 2008; Saitoh *et al.* 2010; Yashiro *et al.* 2010) and in a deciduous broad-leaved forest at the AsiaFlux TKY site (Saigusa *et al.* 2002; Ohtsuka *et al.* 2005, 2009). To reveal differences in the carbon budgets of the two forest types and the major causes of these differences, we used the National Center for Atmospheric Research / Land Surface Model (NCAR/LSM; Bonan 1996), which simulates carbon, energy, and water fluxes. We focused on three points: (1) To improve the model's predictions, we evaluated the effects of model calibration using both the tower flux data and the biometric data from the two sites. (2) To clarify the influence of the growing period length on the carbon budget in the deciduous broad-leaved forest, we investigated the temperature dependency of the forest's plant area index (PAI), because PAI is one of the key biophysical parameters in the model (Bonan 1993) and because the timings of leaf expansion and leaf-fall were correlated well with seasonal changes of air temperature (Polgar and Primack 2011). (3) To compare the carbon budgets in the two forest types and to determine the sensitivity of the model outputs to climatic factors, we evaluated the budgets simulated with the micrometeorological data from each site at the two forest types.

2. Methods

2.1. Site description

The study was conducted at an evergreen coniferous forest site (TKC; 36°08′N, 137°22′E; 800 m a.s.l.) and a deciduous broad-leaved forest site (TKY; 36°08′N, 137°25′E; 1420 m a.s.l.) belonging to the AsiaFlux network (http://asiaflux.net) and the Japan Long-Term Ecological Research network (JaLTER, http://www.jalter.org). The horizontal distance between the sites is about 10 km. Both sites are located near Takayama City, in the central part of Japan's main island. This region has a cool-temperate climate that is influenced by the Asian monsoon. It is characterized by mild, humid springs and autumns; hot, humid summers; and cold, snowy winters (Lee *et al.* 2008). Table 1 summarizes the vegetation and climate characteristics of the sites. PAI shows a clear seasonal pattern in the deciduous broad-leaved forest (Nasahara *et al.* 2008) but shows little seasonality in the evergreen coniferous forest (Saitoh *et al.* 2010). The difference in annual average temperature between the two altitudes (800 and 1420 m a.s.l.) was 2.2°C (Table 1). Saigusa et al. (2002) and Saitoh *et al.* (2010) provide more detailed descriptions of the TKY and TKC sites, respectively.

2.2. Ecosystem model

We used version 1.0 of the NCAR/LSM model (Bonan 1996). Here, we briefly describe the carbon flux calculations. In this model, the carbon budget is divided into CO_2 uptake by photosynthesis and CO_2 release by plant and heterotrophic respiration. Photosynthesis is coupled to stomatal resistance via parameterization of the model based on the models of Farquhar *et al.* (1980) and Collatz *et al.* (1991) for C_3 plants (see Appendix A for a detailed description). CO_2 release by the ecosystem consists of maintenance respiration, growth respiration, and heterotrophic respiration (see Appendix A for a detailed description). The model is driven at an hourly time step by the values of shortwave and longwave radiation, air temperature, wind speed, precipitation, and relative humidity. The outputs used in this study were carbon budget components (i.e., GPP, RE, NEP, NPP, R_{soil}, R_h, and R_{root}; see Appendix A for a detailed description). The micro-meteorological measurements at the TKY and TKC sites were described in Saigusa *et al.* (2002) and Saitoh *et al.* (2010), respectively.

2.3. Model simulations

To improve the model's performance for both forests, we replaced default parameter values with values based on data from our study sites (Table 2). First, we improved the tree height, bottom of canopy, stem biomass, root biomass, PAI, displacement height, and roughness length parameters with measured values at the two sites. Second, we adjusted the maximum rate of carboxylation at 25°C, foliage maintenance respiration at 25°C, stem maintenance respiration at 25°C, root maintenance respiration at 25°C, and the heterotrophic respiration at 10°C and growth respiration parameters, and further calibrated the model, using tower flux data (i.e., seasonal patterns and the annual values of GPP, RE, and NEP) and biometric data (i.e., annual values of NPP, R_{soil}, R_h, and R_{root}) from the evergreen coniferous

forest at the TKC site (simulation 1, described below) and the deciduous broad-leaved forest at the TKY site (simulation 4, described below), respectively. We used the measured and adjusted parameters in our detailed comparison. The values used for calibration of the carbon budget were obtained from previously published data (Saigusa *et al.* 2005; Ohtsuka *et al.* 2007; Saitoh *et al.* 2010; Yashiro *et al.* 2010; Sasai *et al.* 2011).

To compare the carbon budgets between the two forest types, we ran the model under four scenarios: For

Table 1. Summary of the vegetation and climate characteristics at the AsiaFlux TKC and TKY sites, near Takayama City, Japan

	TKC	TKY
Vegetation type	Evergreen coniferous forest	Deciduous broad-leaved forest
Dominant species	*Cryptomeria japonica* D. Don, *Chamaecyparis obtusa* Sieb. et Zucc.(1)	*Betula ermanii* Cham., *Quercus crispula* Blume(d)
Height of the tree canopy	20 to 25 m(a)	13 to 20 m(e)
Tree age	About 40 to 50 years(b)	About 50 years(f)
Annual maximum plant area index (PAI, excluding understory	PAI = 5 m^2 m^{-2} (b)	PAI = 6 m^2 m^{-2} (e)
Forest-floor vegetation	sparse shrubs, herbs, and ferns(c)	evergreen dwarf bamboo [(*Sasa senanensis* (Franch. et Sav.) Rehder](e)
Annual mean air temperature	9.4 °C(c)	7.2 °C(d)
Annual mean rainfall	About 1700 mm(c)	About 2400 mm(d)
Snow period	December to April(c)	December to April(d)

(a) Lee *et al.* (2008), (b) Saitoh *et al.* (2010), (c) Average values from 2006 to 2010,
(d) Ohtsuka *et al* . (2005), (e) Nasahara *et al.* (2008), (f) Saigusa *et al.* (2002)

Table 2. Representative default values and modified values for the parameters used in the model simulation in the evergreen coniferous forest at the TKC site and deciduous broad-leaved forest at the TKY site

	Parameters	Evergreen coniferous forest at the TKC site		Deciduous broad-leaved forest at the TKY site	
		Default	Modified	Default	Modified
Measured parameters	Tree height (m)	17	20.2(a)	20	18.0(e)
	Bottom of canopy (m)	8.5	10.0(a)	11.5	8.0(e)
	Stem biomass (V_{bs}; kg m^{-2})	3.6	26.08(b)	6.2	11.36(e)
	Root biomass (V_{br}; kg m^{-2})	7.2	8.24(b)	12.4	3.23(e)
	Plant area index (PAI; m^2 m^{-2})	4.5 to 5.5	4.6 to 5.1(c)	0.4 to 5.1	0.8 to 5.4(f)
	Displacement height (m)	11.39	15.75(d)	13.40	5.60(g)
	Roughness length (m)	0.94	1.51(d)	1.10	0.10(g)
Adjusted parameters	Max. rate of carboxylation at 25 °C (V_{cmax25}; μmol m^{-2} s^{-1})	33	33	33	40
	Foliage maintenance respiration rate at 25 °C (R_{f25}; μmol m^{-2} s^{-1})	0.5	0.7	0.5	0.3
	Stem maintenance respiration at 25 °C (R_{s25}; μmol kg^{-1} s^{-1})	0.94	0.09	0.02	0.001
	Root maintenance respiration at 25 °C (R_{r25}; μmol kg^{-1} s^{-1})	0.36	0.30	0.01	0.45
	Heterotrophic respiration parameter at 10 °C (a_3; μmol kg^{-1} s^{-1})	0.37	0.37	0.40	0.32
	Proportionality coefficient of Growth respiration (a_{gr})	0.25	0.25	0.25	0.10

(a) Megumi Ishida, unpublished data, (b) Yashiro *et al.* (2010), (c) Saitoh *et al.* (2010), (d) Taku M. Saitoh, unpublished data,
(e) Ohtsuka *et al* . (2005), (f) Nasahara *et al.* (2008), (g) Ichiro Tamagawa, unpublished data

the carbon budget of the evergreen coniferous forest, Simulation 1 used the climatic data recorded in that warmer forest (800 m a.s.l., 2006 and 2007), whereas Simulation 3 used the colder TKY climatic data (1420 m a.s.l., 2002 and 2003). For the carbon budget of the deciduous broad-leaved forest, Simulation 2 used the warmer TKC climatic data (800 m a.s.l., 2006 and 2007), whereas Simulation 4 used the data recorded within the colder deciduous forest (1420 m a.s.l., 2002 and 2003).

We compared simulation 1 with simulation 2 (which had an "expanded growing period" due to the use of warmer temperatures as mentioned below), and simulation 3 with simulation 4. Because PAI of broad-leaved forests depends on growing period length, in simulation 2 we calculated the carbon budget using two different seasonal variations in PAI: one used "modified growing period" based on the measured data at 1420 m a.s.l. (i.e., we assumed no temperature dependency of PAI and used the parameters in Table 2), and the other used adjusted parameters that accounted for the effects of changes in leaf phenology as a function of temperature (i.e., we used an "expanded growing period" that accounted for warmer temperatures at the lower elevation of the TKC site). In simulation 4, we used the seasonal pattern of PAI measured in the deciduous broad-leaved forest at the TKY site as the modified model parameters for PAI (i.e., we used the modified parameters in Table 2). In simulations 1 and 3, we used the seasonal pattern of PAI measured in the evergreen coniferous forest at the TKC site as the model parameters for PAI (i.e., we used the modified parameters in Table 2) at the two altitudes, because PAI exhibits little seasonality in evergreen coniferous forests (Saitoh *et al.* 2010).

3. Results and Discussion

3.1. Model calibration and estimation errors

The simulated seasonal patterns of GPP, RE, and NEP coincided well with the tower-flux measurements at both sites (R^2 0.71–0.97 at the TKC site, 0.90–0.98 at the TKY site; Figs. 1, 2; Table 3). The annual errors in GPP, RE, and NEP ranged from 0.1 to 1.0 Mg C ha^{-1} yr^{-1} (Table 4).

The differences in GPP, RE, and NEP between the model estimate and the measured data, especially during the leaf-expansion and leaf-fall periods, might result from the model's simple treatment of ecophysiological variables such as the maximum carboxylation rate at 25°C (V_{cmax25}) and leaf nitrogen (N) content, both which are key parameters that affect carbon dynamics in terrestrial ecosystems. The NCAR/LSM assumes that the values of V_{cmax25} and leaf N content are constant throughout the year. However, Ito *et al.* (2006) and Muraoka *et al.* (2010) examined the effects of seasonal and inter-annual variations in canopy LAI and V_{cmax25} on the GPP of a cool-temperate deciduous broad-leaved forest, and found seasonal variations in V_{cmax25} that affected GPP. Kosugi *et al.* (2003) also concluded that the description of seasonal

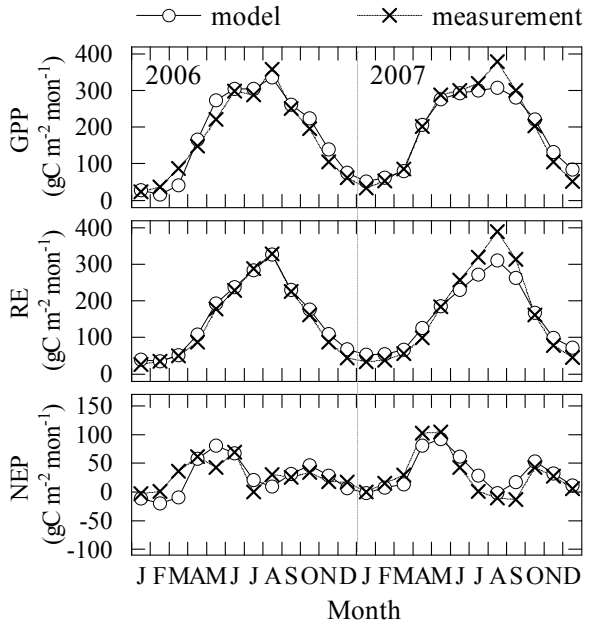

Fig. 1. Comparison between model estimates and measured values of gross primary production (GPP), ecosystem respiration (RE), and net ecosystem production (NEP) in the evergreen coniferous forest at the TKC site from 2006 to 2007.

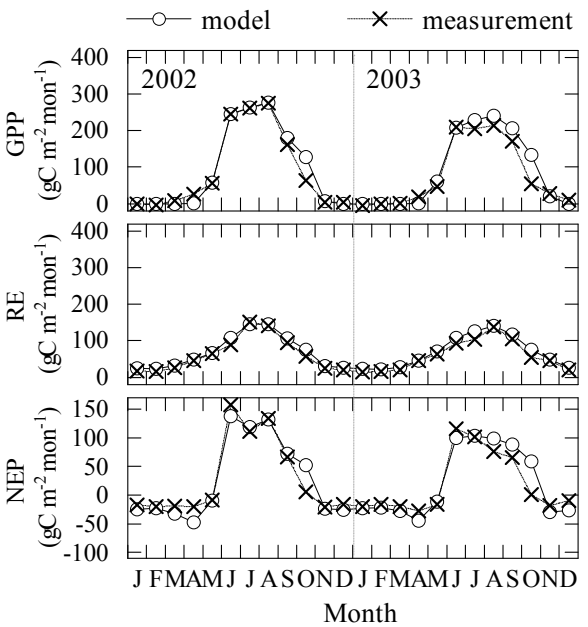

Fig. 2. Comparison between model estimates and measured values of gross primary production (GPP), ecosystem respiration (RE), and net ecosystem production (NEP) in the deciduous broad-leaved forest at the TKY site from 2002 to 2003.

Table 3. Errors in monthly gross primary production (GPP), ecosystem respiration (RE), and net ecosystem production (NEP) simulated by the model in the evergreen coniferous forest at the TKC site and the deciduous broad-leaved forest at the TKY site

		Error (g C m^{-2} mon^{-1})		
Site	Carbon flux	RMSE	MBE	R^2
TKC	GPP	26.7	2.7	0.95
	RE	21.7	1.7	0.97
	NEP	18.0	0.9	0.71
TKY	GPP	24.6	8.4	0.95
	RE	10.6	8.3	0.98
	NEP	19.6	0.1	0.90

RMSE = root-mean-square error;
MBE = mean bias error;
R^2 = coefficient of determination.

physiological changes in V_{cmax25} by a biochemical model of photosynthesis will affect estimates of the long-term CO_2 gas exchange. In addition, Ueyama *et al.* (2010) indicated that the BIOME-BGC model's accuracy of estimation of the carbon budget was improved by accounting for the seasonal pattern of N content in a cool-temperate, deciduous broad-leaved forest. Other studies have reported that N content was not constant throughout the year in evergreen coniferous (e.g., Kobayashi *et al.* 2010) and deciduous broad-leaved (e.g., Wilson *et al.* 2000) forests. These results suggest that some of our estimation errors resulted from the model's failure to account for seasonal variations in V_{cmax25} and N content.

The differences in GPP, RE, and NEP between model estimates and the measured data, especially in summer at the TKC site, might similarly result from the model's parameters for the water cycle. Saitoh *et al.* (2010) reported that soil dryness influenced the maximum GPP estimated by non-linear curve fitting of the relationship between light intensity (photosynthetic photon flux density, PPFD) and GPP in August 2007 at the TKC site. The model might overestimate the effects of soil moisture stress on GPP and RE. To improve the model's accuracy, it will be necessary to calibrate the water budget against field measurements.

Although measurement data are useful for model calibration and validation, it's important to remember that they usually include estimation errors. Previous studies indicated that random measurement errors in estimates of the annual carbon budget by the eddy-covariance approach are typically on the order of ±0.3 to 0.5 Mg C ha^{-1} yr^{-1} (Baldocchi 2003; Richardson and Hollinger 2007). However, the errors sometimes exceed ±1.0 Mg C ha^{-1} yr^{-1} at mountain sites (Baldocchi 2003). Carbon budget estimation based on the eddy-covariance approach has been carefully evaluated at the TKC and TKY sites by means of "quality control and quality assurance" and gap-filling (Saigusa *et al.* 2002; Saitoh *et al.* 2010). These analyses showed that the eddy-covariance measurements have uncertainties due to a potential systematic bias

Table 4. Validation of the simulated (model) annual cumulative carbon fluxes in the evergreen coniferous forest at the TKC site and the deciduous broad-leaved forest at the TKY site. Note that this validation includes some uncertainty arising from the difference in the periods used for the model and the measurement data in (b) and (d)

Site	Carbon flux	Model simulation (Mg C ha^{-1} yr^{-1})	Measurement
TKC	GPP	22.3	22.1[(a)]
	RE	18.9	18.6[(a)]
	NEP	3.5	3.4[(a)]
	NPP	7.7	7.9[(b)]
	R_{soil}	8.3	6.8[(b)]
	R_h	4.1	3.6[(b)]
	R_{root}	4.2	3.3[(b)]
TKY	GPP	11.3	10.3[(c)]
	RE	8.3	7.3[(c)]
	NEP	3.0	2.9[(c)]
	NPP	6.3	6.5[(d)]
	R_{soil}	6.2	6.8[(e)]
	R_h	3.3	3.7[(e)]
	R_{root}	2.9	3.1[(e)]

GPP = gross primary production; RE = ecosystem respiration;
NEP = net ecosystem production;
NPP = net primary production;
R_{soil} = soil respiration; R_h = heterotrophic respiration;
R_{root} = root respiration.
(a) 2-year average from 2006 to 2007 estimated using the tower flux–based (eddy-covariance) method (Saitoh *et al.* 2010).
(b) 4-year average from May 2005 to March 2009 estimated using biometric data (Yashiro *et al.* 2010).
(c) 2-year average from 2002 to 2003 estimated using the tower flux–based (eddy-covariance) method (Saigusa et al. 2005).
(d) 5-year average from 1999 to 2003 estimated using biometric data (Ohtsuka *et al.* 2007).
(e) 2-year average from 2002 to 2003 estimated using biometric data (Ohtsuka *et al.* 2007).

associated with energy-imbalance problems (Wilson *et al.* 2002; Foken 2008) and may also underestimate the nocturnal ecosystem flux under stable atmospheric conditions (van Gorsel *et al.* 2007, 2009). The differences between the modeled and measured carbon fluxes were <1.0 Mg C ha^{-1} yr^{-1}, except for R_{soil} at the TKC site (Table 4). The differences were of the same order of magnitude as the differences in measured NEP between the eddy-covariance and biometric approaches: Hirata *et al.* (2008) compared a tower flux–based NEP with a biometric-based NEP at six Asian forest sites, including the TKY site, and found that the difference (tower flux- biometric) in the NEPs at each site ranged from –1.0 to +1.5 Mg C ha^{-1} yr^{-1}. In addition, Yashiro *et al.* (2010) compared the eddy-covariance and biometric estimates of NEP at the TKC site and found that the two approaches differed by about 1.0 Mg C

ha^{-1} yr^{-1}. We conclude that the simulated carbon budget in our forests was within these levels of measurement error.

Yashiro *et al.* (2010) indicated that the measurement errors in a biometric approach may be caused by (1) an insufficient number of sample points for measurement components such as soil respiration and biomass (mainly due to spatial and temporal heterogeneity of the variables), (2) uncertainty in root growth and respiration, and (3) footprint differences between the tower flux and biometric approaches. For instance, Liang *et al.* (2004) found large differences in CO_2 efflux among four observational approaches. These reports suggest the need for a more robust approach to measuring soil respiration so that this parameter can be divided into root and heterotrophic respiration, and the need to calibrate the relationship between measurements obtained using different instruments.

3.2. Sensitivity analysis of the impact of growing period length on the carbon budget

Using daily canopy surface images and air temperature data at the TKY site (1420 m a.s.l.) from 2004 to 2009 (Nagai *et al.* 2011), we examined the dates of the beginning of leaf expansion, the beginning of autumn leaf color development, and the end of leaf-fall, and their relationships with air temperature. We found that (1) leaf expansion began when the accumulated effective air temperature from the first day of the year (based on a 5°C threshold) exceeded 140.0 ± 13.5°C (average ± standard deviation) during spring; (2) leaf color development began when the 5-day moving-average daily temperature fell below 10.8 ± 1.3°C during autumn; and (3) the leaf-fall period, which was defined as the period between the beginning of autumn leaf color development and the end of leaf-fall, was 30.7 ± 4.0 days.

We adapted these relationships between leaf phenology in the deciduous broad-leaved forest and air temperature to account for the seasonal variation of PAI at the warmer TKC site (800 m a.s.l.). As a result, the beginning of leaf expansion and the end of leaf-fall were 12.7 days earlier and 9.9 days later, respectively, at 800 m a.s.l. than they were at 1420 m a.s.l. In total, the potential growing period was therefore about 23 days longer at the lower altitude. We defined this expanded period of tree phenology as one of the two sets of model parameters for PAI at 800 m a.s.l. In simulation 2, the carbon budget differed between the "modified growing period" and "expanded growing period" simulations: the latter GPP, NPP, and NEP values were 12.7%, 19.0%, and 48.0%, respectively, greater than the "modified growing period" values (Figure 3). The increases were explained mainly by the increased carbon gain during spring and autumn due to expanded growing period (data not shown). This result was supported by long-term measurements at the TKY site from 1994 to 2009: GPP of 10.5 Mg C ha^{-1} yr^{-1} and NEP of 2.4 Mg C ha^{-1} yr^{-1} in years with the highest annual temperature (average values of 7.5°C), in 1998 and 2004, which were considerably larger than the corresponding values of 8.2 and 1.2 Mg C ha^{-1} yr^{-1} in two years with the lowest mean annual air temperature, in 1995 and 1996 (i.e., average values of 5.6°C) (Saigusa *et al.* 2005; Ohtsuka *et al.* 2009).

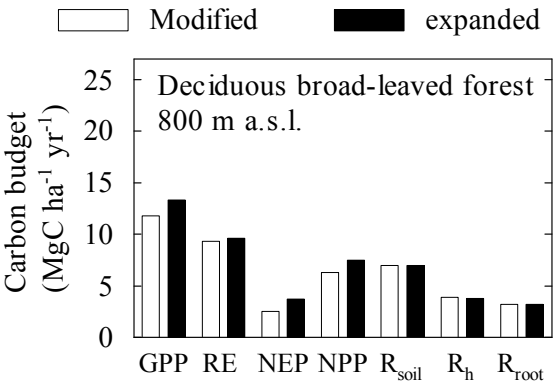

Fig. 3. Annual carbon budget simulated by using "modified growing period" and "expanded growing period" in the deciduous broad-leaved forest under the TKC meteorological conditions. GPP is gross primary production, RE is ecosystem respiration, NEP is net ecosystem production, NPP is net primary production, R_{soil} is soil respiration, R_h is heterotrophic respiration, and R_{root} is root respiration.

3.3. Comparison of the carbon budgets of the two forest types

The simulated GPP of the evergreen coniferous forest was higher than that of the deciduous broad-leaved forest under the climatic conditions at both elevations, especially from April to June (Figures 4, 5). In both forests, the maximum leaf-scale carboxylation rate (V_{cmax}) during spring and early summer was smaller than that during mid-summer (e.g., Kosugi *et al.* 2003; Kosugi and Matsuo 2006; Han *et al.* 2004; Muraoka *et al.* 2010). However, LAI clearly differed between the two forest types from April to June: In Japanese cool-temperate, deciduous broad-leaved forests, leaf expansion begins in April or May and LAI does not reach its maximum value during this period (Nasahara *et al.* 2008). In contrast, evergreen coniferous forests of this region have PAI values from April to June that are similar to those from July to September (Saitoh *et al.* 2010). Therefore, the difference in GPP from April to June may be influenced by differences in the seasonal patterns of PAI between the two forest types.

The difference in GPP between the two forest types from April to June affected the seasonal variation in NEP: NEP peaked from April to June in the evergreen coniferous forest but from July to September in the deciduous broad-leaved forest. Our results confirm previous studies of the seasonal patterns of NEP in evergreen coniferous and deciduous broad-leaved forests in East Asia (e.g., Saigusa *et al.* 2008). In addition, the biomass in the evergreen coniferous forest was more than twice that in the deciduous broad-leaved

forest (Table 2). As a result, under the microclimatic conditions at both altitudes, the annual values of GPP, RE, and light-use efficiency (LUE), which we calculated as the ratio of GPP to PPFD measured at the flux towers in the two forests, were clearly greater in the evergreen coniferous forest than in the deciduous broad-leaved forest, and the differences (coniferous – deciduous) in NEP, NPP, R_{soil}, R_h, and R_{root} between the forests ranged from –0.2 to +2.1 Mg C ha^{-1} yr^{-1} (Figure 5). Our findings suggest that the evergreen coniferous forest has higher metabolic activity than the deciduous broad-leaved forest in this cool-temperate region of Japan.

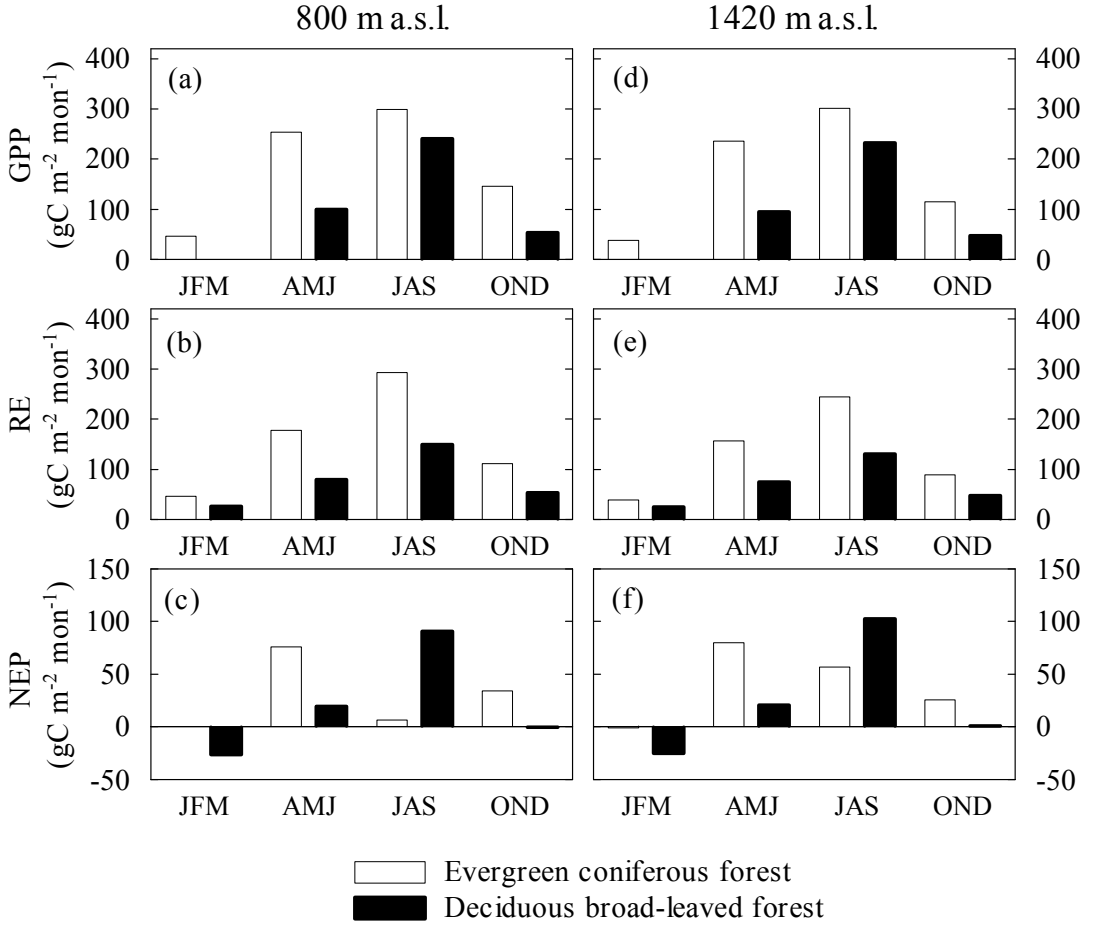

Fig. 4. Comparison of the carbon budget between the evergreen coniferous forest and the deciduous broad-leaved forest under the different meteorological conditions at the two altitudes for four periods during the year. GPP is gross primary production, RE is ecosystem respiration, and NEP is net ecosystem production. JFM, AMJ, JAS, and OND indicate the average values from the corresponding months of the year. Note that "expanded growing period" was used in simulation 2 (the carbon budget in the deciduous broad-leaved forest at 800 m a.s.l.).

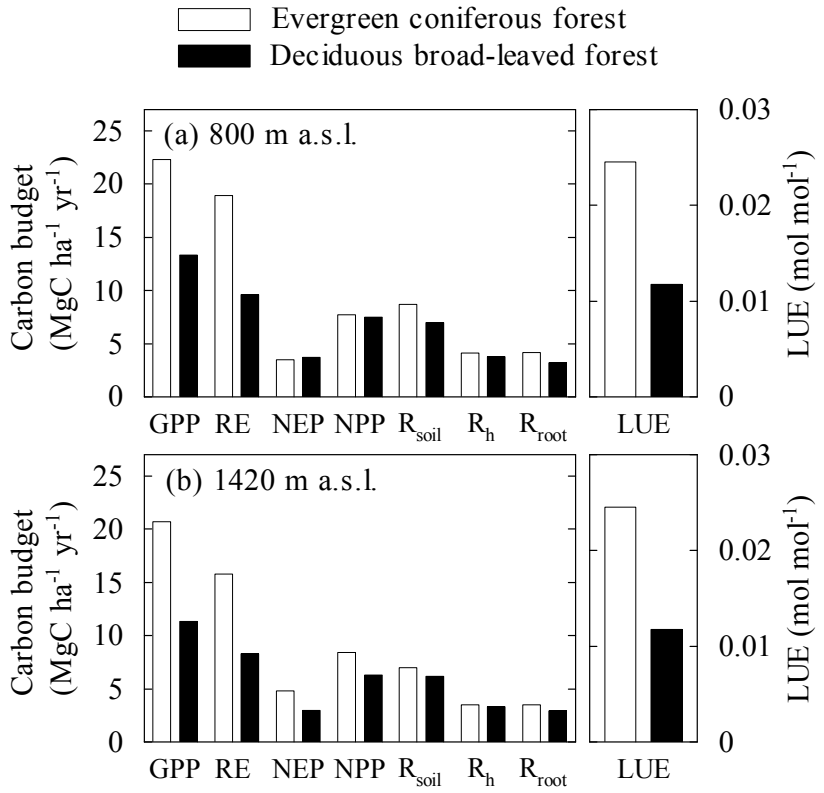

Fig. 5. Comparison of the annual carbon budget and light-use efficency (LUE) between the evergreen coniferous forest and the deciduous broad-leaved forest under the different meteorological conditions at the two altitudes. GPP is gross primary production, RE is ecosystem respiration, NEP is net ecosystem production, NPP is net primary production, R_{soil} is soil respiration, R_h is heterotrophic respiration, and R_{root} is root respiration. Note that "expanded growing period" was used in simulation 2 (the carbon budget in the deciduous broad-leaved forest at 800 m a.s.l.).

3.4. Implications for future studies

This study is the first step in evaluating differences in the carbon budget characteristics between evergreen coniferous and deciduous broad-leaved forests in the cool-temperate region of Japan. Our analytical approach to determining the carbon budgets based on calibration of the simulation model using both tower flux and biometric data can be conducted at various spatial scales. To apply the calibration approach to other ecosystems and to evaluate the carbon budget with improved accuracy from regional to global scales, researchers will require general, long-term, continuous, and comprehensive biometric information, such as NPP and biomass values, and phenological information, such as PAI, from tower flux sites. To achieve this goal, it will be necessary to share ecosystem databases, as has been done by the International Long Term Ecological Research project (ILTER; http://www.ilternet.edu/) and the Phenological Eyes Network (PEN; http://www.pheno-eye.org). It will be also necessary to confirm the present results by determining carbon budgets for the same forest types at three or more elevations or three or more latitudes at the same elevation to confirm the differences as a function of altitude that we observed here.

Recent studies indicate that estimates based on a fine spatial resolution (a 1-km grid) were much more effective for evaluating ecosystem carbon cycles than simulations at a coarser spatial resolution (about a 100-km grid) for landscapes with complex topography (Ito 2008; Sasai *et al.* 2011). Our results revealed clear differences in growing period length and in carbon budget estimates between the two altitudes, even though the horizontal distance between the two sites was less than 10 km. Furthermore, the tree phenology characteristics in deciduous broad-leaved forests at different altitudes clearly affected the carbon budget estimation. Our results therefore indicate the importance of determining the optimal spatial resolution for use in evaluating the carbon budget of regions such as Japan that have complex topography.

Appendix A: Estimation of carbon budget components in NCAR/LSM

NCAR/LSM is a sun and shade model that does not account for the effects of the understory vegetation. The sunlit fraction of the canopy (f_{sun}) is given by:

$$f_{sun} = \frac{\int_0^{L+S} e^{-Kx} dx}{L+S} = \frac{1-e^{-K(L+S)}}{K(L+S)} \qquad (A1)$$

where $e^{-K(L+S)}$ is the fractional area of sunflecks on a horizontal plane below the leaf and stem areas (represented by the indices L and S, respectively), and K represents scattering within canopy. The shaded fraction (f_{shade}) equals [1 – f_{sun}], and the sunlit and shaded LAIs are [L_{sun} = f_{sun} L] and [L_{shade} = f_{shade} L], respectively. Bonan (1996) provides details of the calculation scheme for incident solar radiation at the canopy level and for the energy budget resulting from the radiation and the water vapor balances.

The photosynthesis part of LSM (Bonan 1996) is based on those of Farquhar *et al.* (1980) and Collatz *et al.* (1991). Single-leaf photosynthesis of C_3 plant is determined as:

$$A = \min(w_c, w_j, w_e) \qquad (A2)$$

where w_c is the RuBP carboxylase–limited rate of carboxylation, w_j is the maximum rate of carboxylation allowed by the capacity to regenerate RuBP, and w_e is the export-limited rate of carboxylation:

$$w_c = \frac{\left(c_i - \Gamma^*\right) V_{cmax}}{c_i + K_c\left(1 + \frac{o_i}{K_o}\right)} \qquad (A3)$$

$$w_j = \frac{\left(c_i - \Gamma^*\right) 4.6\,\varphi\,\alpha}{c_i + 2\Gamma^*} \qquad (A4)$$

where φ is the absorbed photosynthetically active radiation calculated in LSM, α is the quantum yield of photosynthesis (μmol CO_2 μmol^{-1} photons), c_i is the initial leaf CO_2 concentration (Pa), Γ^* is the CO_2 compensation point (Pa), o_i is O_2 concentration (Pa), K_c is the Michaelis-Menten constants for CO_2 (Pa), and K_o is the Michaelis-Menten constants for O_2 (Pa). Here, V_{cmax} varies with temperature and soil water as follows:

$$V_{cmax} = V_{cmax25}\, a_{V\max}^{\frac{T_v - 25}{10}} f(N) \beta_t\, f(Tv) \qquad (A6)$$

where V_{cmax25} is the value at 25°C, a_{Vcmax} is a temperature sensitivity parameter for V_{cmax} (fixed at 2.4), T_v is leaf temperature, $f(N)$ is an adjustment parameter for the rate of photosynthesis that accounts for the leaf nitrogen (N) content ($f(N)$ = 1 in this study), β_t varies from 0 to 1 (depending on soil water conditions), and $f(T_v)$ is a function that mimics the thermal breakdown of metabolic processes (Bonan 1996):

$$f(T_v) = \left[1 + \exp\left(\frac{-220000 + 710 \cdot (T_v + 273.16)}{8.314 \cdot (T_v + 273.16)}\right)\right]^{-1} \qquad (A7).$$

The photosynthetic rate in the LSM is determined by iterative calculation of the model defined by equations A1 to A7 and a modified stomatal conductance model:

$$g_{sw} = m \frac{A}{c_s} \frac{e_s}{e_i} P_{atm} + g_0 \qquad (A8)$$

where g_{sw} is the stomatal conductance for water vapor (mol m^{-2} s^{-1}), m is an empirical regression parameter, A is the photosynthetic rate (μmol CO_2 m^{-2} s^{-1}), c_s is the CO_2 concentration at the leaf surface (Pa), e_s is the vapor pressure at the leaf surface (Pa), e_i is the saturation vapor pressure (Pa) inside the leaf at the vegetation temperature, and g_0 is the minimum stomatal conductance (0.002 mol m^{-2} s^{-1}) when A = 0. These calculations are made for both sunlit and shaded parts of the canopy (A_{sun} and A_{shade}) and are summed for the entire canopy as GPP = [$A_{sun} \cdot L_{sun} + A_{shade} \cdot L_{shade}$].

Plant respiration is broken into maintenance and growth respiration. Total maintenance respiration in the LSM is determined by the sum of the foliar (R_{mf}), stem (R_{ms}), and root (R_{mr}) respiration:

$$\begin{aligned} R_m &= R_{mf} + R_{ms} + R_{mr} \\ &= \left[L \cdot R_{f25} \cdot f(N) \cdot \beta_t + V_{bs} \cdot R_{s25} + V_{br} \cdot R_{r25}\right] a_{rm}^{\frac{T_v - 25}{10}} \end{aligned} \qquad (A9)$$

where L is the leaf area index (m^2 m^{-2}), R_{f25} is foliar respiration at 25°C (μmol CO_2 m^{-2} s^{-1}), V_{bs} is stem biomass (kg m^{-2}), R_{s25} is stem respiration at 25°C (μmol CO_2 kg^{-1} s^{-1}), V_{br} is root biomass (kg m^{-2}), R_{r25} is root respiration at 25°C (μmol CO_2 kg^{-1} s^{-1}), and a_{rm} is a temperature sensitivity parameter. Growth respiration (R_g in LSM) is proportional to GPP, as follows:

$$R_g = a_{gr} \cdot GPP \qquad (A10)$$

where a_{gr} is a proportionality coefficient.

Heterotrophic respiration (R_h) is determined by the following equation:

$$R_h = \frac{\theta}{a_1 + \theta} \frac{a_2}{a_2 + \theta} a_3 S_c a_4^{\frac{T_s - 10}{10}} \qquad (A11)$$

where θ is the volumetric soil water content a depth of 1 m (m^3 m^{-3}), a_1 is half of field capacity, a_2 is half of the saturated capacity, S_c is soil carbon to a depth of 1m (kg m^{-2}), a_3 is the respiration rate (μmol CO_2 kg^{-1} s^{-1}) at 10°C, a_4 is a temperature sensitivity parameter, and T_s is the temperature (°C) of the first soil layer.

Finally, NEP, NPP, R_{root}, and R_{soil} were calculated using the following equations:

$$NEP = GPP - RE \qquad (A12)$$

$$NPP = NEP + R_h \quad \text{(A13)}$$

$$R_{root} = R_{mr} + R_g \frac{V_{br}}{V_{bs} + V_{br}} \quad \text{(A14)}$$

$$R_{soil} = R_{root} + R_h \quad \text{(A15)}$$

Acknowledgements

We thank Mr. K. Kurumado and Mr. Y. Miyamoto of the River Basin Research Center, Gifu University, for their support at the Takayama Field Station. We also thank Phenological Eyes Network (PEN; http://www.pheno-eye.org) for providing daily canopy surface images. Thanks are also due to the journal's anonymous reviewers for their thoughtful suggestions. This work was supported by the Japan Society for the Promotion of Science (JSPS) 21st Century Center of Excellence Program (Satellite Ecology, Gifu University), by the JSPS-NRF-NSFC A3 Foresight Program, and by a Global Change Observation Mission (GCOM; PI#102) grant from the Japan Aerospace Exploration Agency. T.M. Saitoh was supported by a Grant-in-Aid for Young Scientists (B) (no. 23710005) from the Ministry of Education, Culture, Sports, Science and Technology of Japan. S. Nagai was supported by the Environment Research and Technology Development Fund (S-9) of the Ministry of the Environment, Japan. H. Muraoka was supported by the JSPS Funding Program for Next Generation World-Leading Researchers (NEXT Program).

References

Baldocchi, D.D. (2003) Assessing the eddy covariance technique for evaluating carbon dioxide exchange rates of ecosystems: past, present and future. Global Change Biol., 9: 479–492.

Baldocchi, D.D. (2008) 'Breathing' of the terrestrial biosphere: lessons learned from a global network of carbon dioxide flux measurement systems. Aust. J. Bot., 56: 1–26.

Bonan, G.B. (1993) Physiological controls of the carbon balance of boreal forest ecosystems. Can. J. For. Res., 23: 1453–1471.

Bonan, G.B. (1996) A Land Surface Model (LSM version 1.0) for Ecological-Hydrological-and Atmospheric Studies: Technical Description and User's Guide. National Center for Atmospheric Research, Boulder, CO. NCAR Technical Note.

Bonan, G.B. (2008) Forest and climate change: forcings, feedbacks, and the climate benefits of forests. Science, 320: 1444–1449.

Collatz, G.J., Ball, J.T., Grivet, C. and Berry, J.A. (1991) Physiological and environmental regulation of stomatal conductance, photosynthesis, and transpiration: a model that includes a laminar boundary layer. Agric. For. Meteorol., 54: 107–136.

Farquhar, G.D., von Caemmerer, S. and Berry, J.A. (1980) A biochemical model of photosynthetic CO_2 assimilation in leaves of C_3 species. Planta (Heidelberg), 149: 78–90.

Foken, T. (2008) The energy balance closure problem: an overview. Ecol. Appl., 18: 1351–1367.

Han, Q., Kawasaki, T., Nakano, T., Chiba, Y. (2004) Spatial and seasonal variability of temperature responses of biochemical photosynthesis parameters and leaf nitrogen content within a *Pinus densiflora* crown. Tree Physiol., 24: 737–744.

Hirata, R., Saigusa, N., Yamamoto, S., Ohtani, Y., Ide, R., Asanuma, J., Gamo, M., Hirano, T., Kondo, H., Kosugi, Y., Li, S.-G., Nakai, Y., Takagi, K., Tani, M. and Wang, H. (2008) Spatial distribution of carbon balance in forest ecosystems across East Asia. Agric. For. Meteorol., 148: 761–775.

Ichii, K., Suzuki, T., Kato, T., Ito, A., Hajima, T., Ueyama, M., Sasai, T., Hirata, R., Saigusa, N., Ohtani, Y. and Takagi, K. (2010) Multi-model analysis of terrestrial carbon cycles in Japan: limitations and implications of model calibration using eddy flux observations. Biogeosciences, 7: 2061–2080.

Ito, A. (2008) The regional carbon budget of East Asia simulated with a terrestrial ecosystem model and validated using AsiaFlux data. Agric. For. Meteorol., 148: 738–747.

Ito, A., Inatomo, M., Mo, W., Lee, M.-S., Koizumi, H., Saigusa, N., Murayama, S. and Yamamoto, S. (2007) Examination of model-estimated ecosystem respiration using flux measurements from a cool-temperate deciduous broad-leaved forest in central Japan. Tellus B, 59: 616–624.

Ito, A., Muraoka, H., Koizumi, H., Saigusa, N., Murayama, S. and Yamamoto, S. (2006) Seasonal variation in leaf properties and ecosystem carbon budget in a cool-temperate deciduous broad-leaved forest: simulation analysis at Takayama site, Japan. Ecol. Res., 21: 137–149.

Ito, A., Saigusa, N., Murayama, S. and Yamamoto, S. (2005) Modeling of gross and net carbon dioxide exchange over a cool-temperate deciduous broad-leaved forest in Japan: Analysis of seasonal and interannual change. Agric. For. Meteorol., 134: 122–134.

Kim, J., Lee, D., Hong, J.Y., Kang, S.Y., Kim, S.J., Moon, S.K., Lim, J.H., Son, Y., Lee, J., Kim, S., Woo, N., Kim, K., Lee, B., Lee, B.L. and Kim, S. (2006) HydroKorea and CarboKorea: cross-scale studies of ecohydrology and biogeochemistry in a heterogeneous and complex forest catchment of Korea. Ecol. Res., 21: 881–889.

Kobayashi, H., Inoue, S. and Gyokusen, K. (2010) Spatial and temporal variations in the photosynthesis-nitrogen relationship in a Japanese cedar (C*ryptomeria japonica* D. Don) canopy. Photosynthetica (Prague), 48: 249–256.

Kosugi, Y., Matsuo, N. (2006) Seasonal fluctuations and temperature dependence of leaf gas exchange parameters of co-occurring evergreen and deciduous trees in a temperate broad-leaved forest. Tree Physiol., 26: 1173–1184.

Kosugi, Y., Shibata, S., Kobayashi S. (2003)

Parameterization of the CO_2 and H_2O gas exchange of several temperate deciduous broad-leaved trees at the leaf scale considering seasonal changes. Plant Cell Environ., 26: 285–301.

Lee, M.-S., Lee, J.-S. and Koizumi, H. (2008) Temporal variation in CO_2 efflux from soil and snow surfaces in a Japanese cedar (*Cryptomeria japonica*) plantation, central Japan. Ecol. Res., 23: 777–785.

Liang, N., Nakadai, T., Hirano, T., Qu, L., Koike, T., Fujinuma, Y. and Inoue, G. (2004) In situ comparison of four approaches to estimating soil CO_2 efflux in a northern larch (*Larix kaempferi* Sarg.) forest. Agric. For. Meteorol., 123: 97–117.

Litton, C.M., Raich, J.W. and Ryan, M.G. (2007) Carbon allocation in forest ecosystems. Global Change Biol., 13: 2089–2109.

Muraoka, H. and Koizumi, H. (2009) Satellite ecology (SATECO)—linking ecology, remote sensing and micrometeorology, from plot to regional scale, for the study of ecosystem structure and function. J. Plant Res., 122: 3–20.

Muraoka, H., Saigusa, N., Nasahara, K.N., Noda, H., Yoshino, J., Saitoh, T.M., Nagai, S., Murayama, S. and Koizumi, H. (2010) Effects of seasonal and interannual variations in leaf photosynthesis and canopy leaf area index on gross primary production of a cool-temperate deciduous broadleaf forest in Takayama, Japan. J. Plant Res., 123: 563–576.

Nagai, S., Maeda, T., Gamo, M., Muraoka, H., Suzuki, R. and Nasahara, K.N. (2011) Using digital camera images to detect canopy condition of deciduous broad-leaved trees. Plant Ecol. Diversity, 4: 78–88.

Nasahara, N.K., Muraoka, H., Nagai, S. and Mikami, H. (2008) Vertical integration of leaf area index in a Japanese deciduous broad leaved forest. Agric. For. Meteorol., 148: 1136–1146.

Ohtsuka, T., Akiyama, T., Hashimoto, Y., Inatomi, M., Sakai, T., Jia, S., Mo, W., Tsuda, S. and Koizumi, H. (2005) Biometric based estimates of net primary production (NPP) in a cool-temperate deciduous forest stand beneath a flux tower. Agric. For. Meteorol., 134: 27–38.

Ohtsuka, T., Mo, W., Satomura, T., Inatomi, M. and Koizumi, H. (2007) Biometric based carbon flux measurements and net ecosystem production (NEP) in a temperate deciduous broad-leaved forest beneath a flux tower. Ecosystems, 10: 324–334.

Ohtsuka, T., Saigusa, N. and Koizumi, H. (2009) On linking multiyear biometric measurements of tree growth with eddy covariance-based net ecosystem production. Global Change Biol., 15: 1015–1024.

Polgar, C.A. and Primack, R.B. (2011) Leaf-out phenology of temperate woody plants: from trees to ecosystems. New Phytol., 191: 926–941.

Richardson, A.D. and Hollinger, D.Y. (2007) A method to estimate the additional uncertainty in gap-filled NEE resulting from long gaps in the CO_2 flux record. Agric. For. Meteorol., 147: 199–208.

Saigusa, N., Yamamoto, S., Hirata, R., Ohtani, Y., Ide, R., Asanuma, J., Gamo, M., Hirano, T., Kondo, H., Kosugi, Y., Li, S.-G., Nakai, Y., Takagi, K., Tani, M. and Wang, H. (2008) Temporal and spatial variations in the seasonal patterns of CO_2 flux in boreal, temperate, and tropical forests in East Asia. Agric. For. Meteorol., 148: 700–713.

Saigusa, N., Yamamoto, S., Murayama, S. and Kondo, H. (2005) Inter-annual variability of carbon budget components in an AsiaFlux forest site estimated by long-term flux measurements. Agric. For. Meteorol., 134: 4–16.

Saigusa, N., Yamamoto, S., Murayama, S., Kondo, H. and Nishimura, S. (2002) Gross primary production and net ecosystem exchange of a cool-temperate deciduous forest estimated by the eddy covariance method. Agric. For. Meteorol., 112: 203–215.

Saitoh, T.M., Tamagawa, I., Muraoka, H., Lee, N.-Y.M., Yashiro, Y. and Koizumi, H. (2010) Carbon dioxide exchange in a cool-temperate evergreen coniferous forest over complex topography in Japan during two years with contrasting climates. J. Plant Res., 123: 473–483.

Sasai, T., Saigusa, N., Nasahara, K.M., Ito, A., Hashimoto, H., Nemani, R., Hirata, H., Ichii, K., Takagi, T., Saitoh, T.M., Ohta, T., Murakami, K., Oikawa, T. and Yamaguchi, Y. (2011) Satellite-driven estimation of terrestrial carbon flux over Far East Asia with 1-km grid resolution. Remote Sens. Environ., 115: 1758–1771.

Sitch, S., Huntingford, C., Gedney, N., Levy, P.E., Lomas, M., Piao, S.L., Betts, R., Ciais, P., Cox, P., Friedlingstein, P., Jones, C.D., Prentice, I.C. and Woodward, F.I. (2008) Evaluation of the terrestrial carbon cycle, future plant geography and climate-carbon cycle feedbacks using five dynamic global vegetation models (DGVMs). Global Change Biol., 14: 2015–2039.

Toda, M., Takata, K., Nishimura, N., Yamada, M., Miki, N., Nakai, N., Kodama, Y., Uemura, S., Watanabe, T., Sumida, A. and Hara, T. (2011) Simulating seasonal and inter-annual variations in energy and carbon exchanges and forest dynamics using a process-based atmosphere–vegetation dynamics model. Ecol. Res., 26: 105–121.

Ueyama, M., Ichii, K., Hirata, R., Takagi, K., Asanuma, J., Machimura, T., Nakai, Y., Ohta, T., Saigusa, N., Takahashi, Y. and Hirano, T. (2010) Simulating carbon and water cycles of larch forests in East Asia by the BIOME-BGC model with AsiaFlux data. Biogeosciences, 7: 959–977.

van Gorsel, E., Delpierre, N., Leuning, R., Black, A., Munger, W.J., Wofsy, S., Aubinet, M., Feigenwinter, C., Beringer, J., Bonal, D., Chen, B., Chen, J., Clement, R., Davis, K.J., Desai, A.R., Dragoni, D., Etzold, S., Grünwald, T., Gu, L., Heinesch, B., Hutyra, L.R., Jans, W.W.P., Kutsch, W., Law, B.E., Leclerc, M.Y., Mammarella, I., Montagnani, L., Noormets, A., Rebmann, C. and Wharton, S. (2009) Estimating nocturnal

ecosystem respiration from the vertical turbulent flux and change in storage of CO_2. Agric. For. Meteorol., 149: 1919–1930.

van Gorsel, E., Leuning, L., Cleugh, H.A., Keith, H. and Suni, T. (2007) Nocturnal carbon efflux: reconciliation of eddy covariance and chamber measurements using an alternative to the u*-threshold filtering technique. Tellus B, 59: 397–403.

Wilson, K.B., Baldocchi, D.D., and Hanson, A.P.J. (2000) Spatial and seasonal variability of photosynthetic parameters and their relationship to leaf nitrogen in a deciduous forest. Tree Physiol., 20: 565–578.

Wilson, K., Goldstein, A., Falge, E., Aubinet, M., Baldocchi, D., Berbigier, P., Ceulenmans, R., Dolman, H., Field, C., Grelle, A., Ibrom, A., Law, B.E., Lowalski, A., Meyers, T., Moncrieff, J., Monson, R., Oechel, W., Tenhinen, J., Valentini, R. and Verma, S. (2002) Energy balance closure at FLUXNET sites. Agric. For. Meteorol., 113: 223–243.

Xue, B.-L., Kumagai, T., Iida, S., Nakai, T., Matsumoto, K., Komatsu, H., Otsuki, K. and Ohta, T. (2011) Influences of canopy structure and physiological traits on flux partitioning between understory and overstory in an eastern Siberian boreal larch forest. Ecol. Modell., 222: 1479–1190.

Yashiro, Y., Lee, N.-Y., Ohtsuka, T., Shizu, Y., Saitoh, T.M. and Koizumi, H. (2010) Biometric based estimation of net ecosystem production (NEP) in a mature Japanese cedar (*Cryptomeria japonica)* plantation beneath a flux tower. J. Plant Res., 123: 463–472.

Yu, G.-R., Wen, X.-F., Sun, X.-M., Tanner, B.D., Lee, X.H. and Chen, J.-Y. (2006) Overview of ChinaFLUX and evaluation of its eddy covariance measurement. Agric. For. Meteorol., 137: 125–137.